

Tetrapeptide Melanocortin Agonist Ligands  
Exploring Selectivity of the mMC3R Using DPhe  
Substitutions in the Ac-His-Arg-DPhe-Tic-NH<sub>2</sub>  
Scaffold

A THESIS SUBMITTED TO THE FACULTY OF THE  
UNIVERSITY OF MINNESOTA BY

Katherine N. Schlasner

Dr. Carrie Haskell-Luevano

March 2018

Copyright: Katherine Schlasner 2018

## Abstract

There are five melanocortin receptors (MC1R-MC5R) that primarily activate the signaling pathway for adenylate cyclase. While both the MC3R and MC4R are hypothesized to be involved in regulating energy homeostasis, the MC3R functionality has been elusive to characterize due to the lack of MC3R-selective ligands. The melanocortin system has been clearly defined as a target for treating obesity or cachexia. When centrally delivered through intracerebroventricular administration, agonists decrease food intake, while antagonists increase food intake. Previous weight management therapies have focused on targeting the MC4R, though off-target cardiovascular effects may limit the clinical utility of these ligands. Therefore, obtaining a MC3R selective compound may allow for a weight regulation therapy that will not have the same cardiovascular liabilities.

MC4R-selective ligands have been heavily investigated, however MC3R-selective ligands have largely gone unexplored. A mixture-based positional scan was conducted to generate scaffolds with MC3R selectivity. The lead compound from the study was Ac-His-Arg-(pI)DPhe-Tic-NH<sub>2</sub>, an MC3R agonist (EC<sub>50</sub> 40nM) and an MC4R antagonist (pA<sub>2</sub> 7.2). The scaffold reverses the sequence of arginine and phenylalanine residues in the His-Phe-Arg-Trp conserved sequence found in endogenous melanocortin ligands. This work presents a follow-up study investigating the position of the phenylalanine residue in efforts to create a MC3R selective agonist with decreased MC4R antagonist activity.

## Acknowledgements

I would like to give a special thanks to my lab mates, because without them this would not have been possible. Thank you to my committee members, Dr. Johnson, Dr. Ambrose, Dr. Pomerantz, and Dr. Doran, for their feedback and support. Special thanks to my advisor, Dr. Carrie Haskell-Luevano for her guidance and encouragement.

## Table of Contents

Acknowledgements.....	ii
List of Tables .....	iv
List of Figures .....	v

### **Exploring mMC3R Activity through SAR of the DPhe position in the Ac-His-Arg-DPhe-Tic-NH<sub>2</sub>**

Introduction.....	Pg. 1
Experimental.....	Pg. 4
Results.....	Pg. 8
Discussion and Conclusion.....	Pg. 12
Bibliography.....	Pg. 27

## List of Tables

<b>Table 1.</b> Tetrapeptide Characterization.....	Pg. 17
<b>Table 2.</b> Agonist and Antagonist Activity of DPhe Substitutions at the mMC3R, mMC4R and mMC5R .....	Pg. 18
<b>Table 3.</b> Agonist Activity of DPhe Substitutions at the mMC1R.....	Pg. 20
<b>Table 4.</b> Calculated Properties of Tetrapeptides.....	Pg. 21

## List of Figures

<b>Figure 1.</b> Scaffold of peptide library .....	Pg 22
<b>Figure 2.</b> Illustration of agonist activity observed in mouse melanocortin-3 receptor.....	Pg 23
<b>Figure 3.</b> Illustration of agonist activity observed in mouse melanocortin-4 receptor.....	Pg 24
<b>Figure 4.</b> Illustration of antagonist activity observed at the mouse melanocortin-4 receptor from the most potent-MC3R agonists.....	Pg 25
<b>Figure 5.</b> Illustration of antagonist activity observed at the mouse melanocortin-4 receptor compounds <b>4, 5, 7</b> .....	Pg 26
<b>Figure 6.</b> Electrostatic Potentials calculated with Maestro.....	Pg 27
<b>Figure 7.</b> A scatterplot showing the potential trend between partition coefficient of octenol over water and mMC3R EC <sub>50</sub> values.....	Pg 28

## **Introduction**

The melanocortin receptor system contains five subtypes labeled MC1R through MC5R, which belong to the class-A family of rhodopsin-like G-protein coupled receptors<sup>1-6</sup>. These receptors primarily signal through the G<sub>αs</sub> subunit, increasing production of cyclic adenosine monophosphate (cAMP)<sup>1-6</sup>. The MC1R is primarily involved in regulation of skin pigmentation<sup>1,6</sup>. The MC2R is only activated by adrenocorticotrophic hormone (ACTH) and is implicated in steroidogenesis<sup>1</sup>. Both the MC3R and MC4R contribute to the regulation of energy homeostasis, which have made them targets for weight regulation therapies<sup>4, 5, 7-10</sup>. Several single nucleotide polymorphisms (SNPs) in the MC4R<sup>11</sup>, and double variants<sup>12</sup> as well as mutations in the MC3R have been associated with the onset of severe obesity<sup>13</sup>. The MC5R functionality in humans is still unknown, but it is known to affect the exocrine gland function in mice<sup>3, 14</sup>.

Endogenous agonists are derived from the proopiomelanocortin (POMC) gene and include  $\alpha$ -,  $\beta$ -, and  $\gamma$ -melanocortin stimulating hormone (MSH) and adrenocorticotrophic hormone (ACTH). The only agonist to stimulate all five receptor subtypes is ACTH;  $\alpha$ -,  $\beta$ -,  $\gamma$ -MSH stimulate all known receptors except the MC2R<sup>2, 15</sup>. The His-Phe-Arg-Trp motif has been found to be the minimum sequence of endogenous agonists necessary for melanocortin activation<sup>16-18</sup>. The melanocortin system contains two naturally occurring antagonists, agouti-signaling protein (ASP), and agouti-related protein (AGRP). The antagonists inhibit receptor function at the MC1, MC3 and MC4 receptors<sup>19-21</sup>. Further studies on AGRP identified the Arg-Phe-Phe motif, as critical for antagonist pharmacology<sup>22</sup>.

Targeting the MC3R/MC4R can lead to development of treatments for metabolic diseases such as obesity, anorexia, and cachexia. When administrated through intracerebroventricular injection (ICV), agonists that are nonselective for the MC3R and MC4R result in decreased food intake<sup>23</sup>. When an endogenous antagonist such as AGRP is administrated in mice it has orexigenic effects, or increased appetite, which can last upward of seven days<sup>24</sup>. While both receptors have a

role in energy homeostasis, the differences in phenotype of knockout mice suggest that these roles are nonredundant. The MC4R knockout models show hyperphagia, they gain fat mass, and experience both weight and length gains compared to wild type mice<sup>25</sup>. Comparatively, the MC3R knockout mice models exhibit increased fat mass and reduced lean mass, while maintaining similar body weight to wild type mice<sup>25</sup>. To further support the hypothesis of independent roles, phenotypic differences between the extremely obese double knockouts and the obese single knockout models have been observed<sup>25</sup>.

Previous clinical trials treating obesity with MC4R drugs and follow up studies reported the side effects of hypertension and induced penile erection<sup>26-30</sup>. Many studies have attempted to determine how the melanocortin receptors and blood pressure are linked<sup>27, 29, 31</sup>. Some evidence indicates that the cardiovascular side effects seen are moderated primarily through the MC4R pathway, with very little contributions from the MC3R pathway<sup>27</sup>. This has been tested by central administration of  $\alpha$ -MSH and  $\gamma$ -MSH, which are more selective for the MC4R and MC3R respectively<sup>27</sup>. When ICV injections of  $\alpha$ -MSH are given, the elevated blood pressure seen in wild type mice is not seen in MC4R deficient mice<sup>27</sup>. The  $\gamma$ -MSH contributions to elevated blood pressure have been thought to be independent of MC3R activity<sup>27</sup>. However, current clinical trials of the peptide Setmelanotid (Ac-Arg-c[Cys-D-Ala-His-D-Phe-Arg-Trp-Cys]-NH<sub>2</sub>), which targets the MC4R, have seen no indication of the adverse cardiovascular side effects<sup>32</sup>. Further exploring the mechanistic differences between the MC3R and MC4R, with compounds of different pharmacological profiles can help in the discovery of weight management therapies that do not have adverse cardiovascular side-effects.

While MC4R-selective agonists have been well studied as possible treatments for metabolic disease, MC3R-selective targets are. Previously reported selective compounds for the MC3R over the MC4R, have primarily been analogues of the endogenous ligands  $\alpha$ - and  $\gamma$ -MSH<sup>33-36</sup>. In hopes of finding scaffolds with more drug-like properties, a mixture-based positional scan was previously used to rapidly scan for new scaffolds with unique pharmacology<sup>37, 38</sup>. Mixture-

based positional scans are a method used to efficiently and systematically explore chemical space<sup>39, 40</sup>. In mixture-based positional scans, multiple compounds are assayed in one well, each of the compounds in the well share the same amino acid residue in a single position. The compounds that are in active mixtures can be synthesized and tested individually. Previously, mixture-based positional scanning has successfully been used to identify tetrapeptides that rescued functionality in human MC4R containing SNPs<sup>41</sup>, and tetrapeptides with unique pharmacology profiles<sup>38</sup>. Amongst the new scaffolds discovered was one of particular interest, Ac-His-Arg-(pI)DPhe-Tic-NH<sub>2</sub>, a MC3R agonist (EC<sub>50</sub> = 40nM) and a MC4R antagonist (pA<sub>2</sub> = 7.0)<sup>37</sup>. This scaffold reverses the sequence of arginine and phenylalanine residues in the His-Phe-Arg-Trp conserved sequence found in endogenous melanocortin ligands<sup>37</sup>.

As compared to the MC3R agonist and MC4R antagonist profile seen by Ac-His-Arg-(pI)DPhe-Tic-NH<sub>2</sub>, the tetrapeptide Ac-His-(pI)DPhe-Arg-Trp-NH<sub>2</sub> expresses partial agonist/antagonist pharmacology at the MC3R and is a full agonist at the MC4R<sup>37</sup>. Previous SAR centered around substitutions of the DPhe residues have been shown that this residue is critical in determining if melanocortin ligands exhibit MC3R or MC4R antagonism<sup>42</sup>. When DPhe was replaced with bulkier residues, DNal(2') and (pI)DPhe, in the synthetic agonist MTII (Ac-Nle-c[Asp-His-DPhe-Arg-Trp-Lys]-NH<sub>2</sub>), potent synthetic MC3R/MC4R antagonists were created<sup>42</sup>. Similarly, exploring substitutions on the DPhe residue in Ac-His-DPhe-Arg-Trp-NH<sub>2</sub> sequence showed that the DPhe residue was extremely important in switching the mMC3R functionality from an agonist to an antagonist<sup>37</sup>. Due to the importance of DPhe in the pharmacological profile of previous melanocortin ligands, it was hypothesized that the (pI)DPhe position in Ac-His-Arg-(pI)DPhe-Tic-NH<sub>2</sub> could be important to the selectivity of agonist activity in the MC3R receptor when compared with MC4R activity.

Herein, we present a SAR that investigates physicochemical properties responsible for the selectivity of the mMC3R agonism over mMC4R activity. The creation of an MC3R selective agonist with decreased agonist and antagonist activity at the MC4R would allow for a chance to

more effectively probe the activity of the MC3R *in vivo* and to develop MC3R selective therapeutics.

## **Experimental**

### *Synthesis:*

Peptides were synthesized using standard solid-phase fluorenyl-9-methyloxycarbonyl (Fmoc) methodology<sup>43, 44</sup>. Couplings were performed using a CEM Discover SPS microwave peptide synthesizer. The 4-(2',4'-dimethoxyphenyl-Fmoc-aminomethyl)phenoxyacetyl-MBHA resin [Rink-amide-MBHA (100-200 mesh), 0.66 mequiv/g substitution], 2-(1H-benzotriazol-1-yl)-1,1,3,3-tetramethyluronium hexafluorophosphate (HBTU), and the listed Fmoc-protected amino acids [Fmoc-His(Trt), Fmoc-Arg(Pbf), Fmoc-(pF)DPhe, and Fmoc-(pCl)DPhe] were purchased from Peptides International (Louisville, KY, USA). The Fmoc-(pBr)DPhe, Fmoc-(3,4-diCl)DPhe, Fmoc-(pCN)DPhe, Fmoc-(pMe)DPhe, Fmoc-p(NH<sub>2</sub>)DPhe(Boc), Fmoc-(pBz)-DPhe, and Fmoc-(4-tBu)DPhe were acquired from BACHEM (San Carlos, CA, USA). Fmoc-(pI)DPhe was procured from Alfa Aesar (Tewksbury, MA, USA). Fmoc-(pCF<sub>3</sub>)DPhe, and Fmoc-(3-Cl)DPhe was bought from Chem Cruz (Dallas, TX, USA). Fmoc-D-4,4'-Biphenylalanine and Fmoc-D-1,2,3,4-tetrahydroisoquinoline-3-carboxylic acid (Tic) were purchased from Synth Tech (Albony, OR, USA). Fmoc-D-Tyr(But) was acquired from Ad. Chem (Louisville, KY, USA). The triisopropylsilane (TIS), *N,N*-diisopropylethylamine (DIEA), 1,2-ethanedithiol (EDT), piperidine, pyridine, and TFA were purchased from Sigma-Aldrich (St. Louis, MO). Acetonitrile (MeCN), *N,N*-dimethylformamide (DMF), dichloromethane (DCM), methanol (MeOH), and acetic anhydride were purchased from Fisher Scientific. All reagents were ACS grade or higher and used without further purification.

Peptides were synthesized from C-terminus to N-terminus on Rink-amide-MBHA resin (Peptides International, 0.66 mequiv/g) in a fritted polypropylene reaction vessel (25 mL CEM reaction vessel). Resin was swelled in DCM for at least 1 hour. Deprotection of the Fmoc protected amino acids was completed using 20% piperidine in DMF at 23°C for two minutes. A second

aliquot of 20% piperidine was added to ensure full deprotection through the assistance of microwave heating (75°C, 30W, 4 min). Amide bonds were formed by adding Fmoc-amino acids, HBTU, and DIEA. After each deprotection or coupling, resin was washed 3-5 times with DMF and confirmed with either a ninhydrin<sup>45</sup> or chloranil test<sup>46</sup>. Ninhydrin/Kaiser tests indicate the presence or lack of a free primary amine and chloranil tests indicate the presence or lack of a secondary amine. After the final peptide was added, the peptide was deprotected a final time and the N-terminus was acetylated on resin using a 3:1 mixture of acetic anhydride:pyridine.

Coupling conditions for the microwave synthesizer were as follows: 3.1:3:5 amino acid:HBTU:DiPEA. N-terminals were acetylated using a 3:1 solution of acetic acid anhydride:pyridine for 30 minutes at room temperature. Peptides were cleaved in a 91:0.3:0.3:0.3 TFA:Thioanisole:TIS:H<sub>2</sub>O mixture. The peptide KNS2-23-9 (Ac-His-Arg-DTyr-Tic-NH<sub>2</sub>) was cleaved in 91:0.3:0.3:0.3 TFA:EDT:TIS:H<sub>2</sub>O mixture. After cleavage, peptides were precipitated in 0°C chilled diethyl ether. The precipitated peptide was pelleted in a centrifuge (Sorvall Legend XTR) at 4000 rpm at 4°C for 4 minutes. The peptide was washed with diethyl ether and pelleted at least three times before drying overnight in a desiccator.

The peptides were purified using RP-HPLC semipreparative chromatography in 0.1% TFA and H<sub>2</sub>O with a C18 reverse phase column. The collected fractions were concentrated on a rotary evaporator and lyophilized three times. The pure compounds were characterized analytically using RP-HPLC with two solvent systems. Both acetonitrile and methanol 10-90% gradients were run in 0.1% TFA in water for 35 min. By integrating the area under the curve at 214 nm purity was determined for each compound. The mass was confirmed using ESI/TOF-MS (Bruker, BioTOF II, University of Minnesota Department of Chemistry Mass Spectrometry Laboratory). The peptide library was named TaMALES, for tetrapeptide melanocortin agonist ligands to explore selectivity.

*Activity:*

***β*-galactosidase assay**

The purified compounds were tested for cAMP activity using a 96-well colorimetric  $\beta$ -galactosidase assay for agonist activity at the MC3R, MC4R, and MC5R and antagonist activity<sup>47</sup> at the MC4R. All  $\beta$ -galactosidase assays were conducted by Dr. Skye Doering. The melanocortin receptors are cloned into HEK293 cells using a pCDNA vector which was previously described<sup>38</sup>. Stably transfected HEK293 cells were plated with Dulbecco's Modified Eagle Medium (DMEM), with 10% bovine serum and 1% penicillin-streptomycin, into a 10 cm dish and grown until 40% confluent. When the cells reached 40% confluency (approximately 24 h later), cells were transiently transfected with 4  $\mu$ g of CRE-PBKS per 10 cm plate of cells using calcium phosphate<sup>48</sup>. Twenty-four hours after the transfection, the cells were plated onto collagen treated Nunclon Delta Surface 96-well plates (Thermo Fischer Scientific) and incubated at 37 °C at 5% CO<sub>2</sub>. Plates were stimulated 48 h post transfection with compounds, which were dissolved in H<sub>2</sub>O and stored at 1000  $\mu$ g/mL in -20°C. They were then incubated at 37°C with 5% CO<sub>2</sub> for 6 hours. Compounds were serially diluted in assay media (1.0 mL 1% bovine serum albumin [BSA] in phosphate buffered saline [PBS] and 1.0 mL of 100x isobutylmethylxanthine in 98.0 mL of DMEM) to concentrations ranging from 10<sup>-4</sup> and 10<sup>-10</sup> M. Positive controls included NDP-MSH (10<sup>-6</sup> to 10<sup>-12</sup> M) and forskolin (10  $\mu$ M). Plain assay media was used as a negative control. After stimulation, media was aspirated from the plates and 50  $\mu$ L of lysis buffer (250 mM Tris-HCL pH=8.0, 740 mL of DDH<sub>2</sub>O, 10 mL of 10% Triton X-100 in water) was added to each well. Plates were stored at -80 °C for up to two weeks, until they were ready to be assayed.

Thawed plates were assessed for protein content and assayed for activity. Protein concentration was determined by adding 10  $\mu$ L of cell lysate to 200  $\mu$ L of BioRad dye solution (1:4 dilution with water) in a new 96-well plate. Absorbance was measured using a 96-well plate reader (Molecular Devices) at  $\lambda = 595$  nm. In order to determine  $\beta$ -galactosidase activity, 40  $\mu$ L of 0.5% BSA in PBS at 37°C, and 150  $\mu$ L of the  $\beta$ -galactosidase substrate (60 mM Na<sub>2</sub>HPO<sub>4</sub>, 1 mM MgCl<sub>2</sub>, 10 mM KCl, 50 mM 2-mercaptoethanol, and 660  $\mu$ M 2-nitrophenyl  $\beta$ -D-galactosidase) were added to the remaining 40  $\mu$ L of cell lysate. Plates were incubated at 37°C and periodically read on the

96-well plate reader until the absorbance at  $\lambda = 405$  nm reached approximately 1.0 relative absorbance units for the positive controls. Each compound was run in duplicate and three independent experiments were completed. All data was fitted with dose-response curves and  $EC_{50}$  values that were calculated using GraphPad Prism v4.0 software.

### **AlphaScreen Bioassay.**

This bioassay was used to determine dose-response curves for compounds at the mMC1R. All AlphaScreen assays were conducted by Katie Freeman. The melanocortin receptors are cloned into HEK293 using a pCDNA vector. AlphaScreen (PerkinElmer) uses a direct measurement of cAMP signaling as previously described. Cells were grown in an incubator at 37°C with 5% CO<sub>2</sub> in cell media [Dulbecco's Modified Eagle's Medium (DMEM) containing 10% newborn calf serum (NCS) and 1% penicillin-streptomycin] in 10 cm plates to 70-95% confluency.

Cells were disassociated with 1 mL of 37°C Versene solution (Gibco), resuspended in 5 mL of 37°C cell media and centrifuged (Sorvall Legend XTR centrifuge, swinging bucket rotor) at 800 rpm for 5 min at RT. The cell pellet was resuspended in Dulbecco's Phosphate Buffered Saline solution (DPBS 1x without CaCl<sub>2</sub> or MgCl<sub>2</sub>, Gibco) warmed to 37°C. A hemocytometer was used to manually count the cells using 10  $\mu$ L of cell mixture added to 10  $\mu$ L of Trypan blue BioRad dye. The cells were centrifuged (800 rpm, 5 min, RT), and the pellet was resuspended in stimulation buffer [Hank's Balanced Salt Solution (HBSS 10x without NaHCO<sub>3</sub> or phenol red, Gibco), 0.5 mM isobutylmethylxanthine (IBMX), 5 mM HEPES buffer solution (1M, Gibco), and 0.1% BSA in Milli-Q water, pH = 7.4] to a final concentration of 10000 cells/ $\mu$ L. A solution of cells and anti-cAMP acceptor beads in stimulation buffer was then prepared (1000 cells/ $\mu$ L and 0.5  $\mu$ g/ $\mu$ L AlphaScreen anti-cAMP acceptor beads in stimulation buffer). Each 384-well microplate (OptiPlate-384, PerkinElmer) contained 10  $\mu$ L of the cell/acceptor bead solution along with 5  $\mu$ L of unknown compounds. Each ligand was tested from concentrations 10<sup>-4</sup> to 10<sup>-12</sup> M. The plate was sealed and incubated at room temperature in the dark for 2 h. Controls included NDP-MSH (10<sup>-6</sup> to 10<sup>-12</sup>), forskolin (10<sup>-4</sup>) and the negative control, stimulation buffer.

The biotinylated cAMP/streptavidin coated donor bead mixture in lysis buffer (0.5  $\mu\text{g}/\mu\text{L}$  AlphaScreen donor beads and 0.62  $\mu\text{M}$  AlphaScreen cAMP biotinylated tracer in a solution of 10% Tween-20, 5 mM HEPES, and 0.1% BSA in Milli-Q water, pH = 7.4) was prepared under green light. Following the initial incubation, 10  $\mu\text{L}$  of the biotinylated cAMP/streptavidin donor bead lysis buffer was added to each well. The plate was resealed and incubated for a second 2 h period in the dark. Post incubation, the plates were read by an EnSpire Alpha plate reader (PerkinElmer). Each compound was run in duplicate and three independent experiments were completed.

### *Physical Properties*

Physical and electrostatic properties of the ligands were determined by using Maestro version 10.4.017 (Schrödinger, LLC, New York, NY, 2015). Charges were assigned using the LigPrep tool at pH 7.4. The ligand was minimized using OPLS 2005 force field<sup>49</sup> until there was a convergence energy difference of 0.0001. The Poisson-Boltzmann equation of electrostatics was implemented where the solvent dielectric constant  $\epsilon = 80$  and the dielectric constant of solute was  $\epsilon = 10$ . Qikprop was used to determine Van der Waals energy,  $\log P_{\text{o/w}}$ , PSA, hydrogen bond donors, and hydrogen bond acceptors.

## **Results**

### *SAR Study*

Substituents of the DPhe residue spanning a variety of electronic and physiochemical properties were tested for *in vitro* melanocortin receptor activity in the tetrapeptide template: Ac-His-Arg-DPhe-Tic-NH<sub>2</sub>. The compounds were manually synthesized using a CEM Discover SPS microwave peptide synthesizer and standard Fmoc solid-phase peptide synthesis procedure<sup>43</sup>. Purification of compounds was completed using semipreparative reverse phase high pressure liquid chromatography (Table 1). Compounds were characterized through ESI-MS, confirming the mass, and RP-HPLC, verifying that all ligands are > 95% pure. Compounds activity was tested at the mouse MC3R-MC5R using a colorimetric  $\beta$ -galactosidase assay that measures cAMP activity (Table 2)<sup>50</sup>. Table 3 summarizes the activity at the mMC1R compounds which was characterized

by measuring intracellular cAMP using the Amplified Luminescent Proximity Homogenous Assay Screen (AlphaScreen, PerkinElmer). The AlphaScreen assay was conducted on mMC1R instead of the *B*-galactosidase assay because the mMC1R cell lines tend to be more impacted by the transfection conditions and duration of the  $\beta$ -galactosidase assay in comparison to the AlphaScreen. The increased stress levels alter the cells cAMP production. Both the  $\beta$ -galactosidase and AlphaScreen assays used stably transfected HEK293 cells expressing the cloned melanocortin receptor.

The tetrapeptide Ac-His-Arg-(p-I)DPhe-Tic-NH<sub>2</sub> was found in a mixture based positional scan and contains a unique mixed pharmacology mMC3R agonist activity ( $EC_{50} = 40$  nM) and mMC4R antagonist activity ( $pA_2 = 7.0$ )<sup>37, 38</sup>. The Ac-His-Arg-(p-I)DPhe-Tic-NH<sub>2</sub> compound was used as a control and had mMC3R agonist activity ( $EC_{50} = 13$  nM) and mMC4R antagonist activity ( $pA_2 = 7.2$ ). The  $EC_{50}$  values of the control are slightly different from literature because the current values were determined through measuring activity using the  $\beta$ -galactosidase assay at the mMC3R mMC4R and mMC5R, while the literature uses the AlphaScreen assay at all tested receptors. Using the two following compounds: Ac-His-Arg-(4,4')DBip-Tic-NH<sub>2</sub> (**1**), Ac-His-Arg-DPhe(p-tBu)-Tic-NH<sub>2</sub> (**2**), were equipotent at the mMC3R ( $EC_{50} < 16$  nM) to the Ac-His-Arg-(p-I)DPhe-Tic-NH<sub>2</sub> (Figure 2, Table 2). Any agonist  $EC_{50}$  values with less than three-fold difference between them are defined to be within experimental error. Compounds **1**, and **2** were all less potent antagonists at the mMC4R ( $6.1 < pA_2 < 6.8$ ) compared to the control compound. All of the compounds have low nanomolar to sub-nanomolar potency at the mMC1R (Table 3) and mMC5R (Table 2). All of nanomolar potent mMC3R compounds showed partial agonist activity at the mMC4R (Figure 3), with the exception of compound **2**, compound **4**, and compound **7** which did not have any mMC4R activity at 100,000 nM (Table 2). This shows that the modified DPhe position in the His-Arg-(pI)DPhe-Tic scaffold can create mMC3R nanomolar agonists and mMC4R partial agonists, this pharmacological profile was previously seen in compounds containing the Arg-(pI)DPhe scaffold<sup>37</sup>. This pharmacological profile is the opposite of that seen when the DPhe position was modified in

the His-DPhe-Arg-Trp scaffold, which created mMC4R agonists that retained nanomolar potency and mMC3R partial agonists/antagonists<sup>51</sup>. This evidence supports the hypothesis that the switching of the DPhe and the Arg residues in His-DPhe-Arg-Trp scaffold can lead to a switch in selectivity between the mMC3R and the mMC4R.

All substituted compounds were more potent than the Ac-His-Arg-DPhe-Tic-NH<sub>2</sub> compound (Table 2). The two compounds that were equipotent to the control were compounds **1** and **2**. Compound **1** has agonist activity at the mMC1R ( $EC_{50} = 0.8 \pm 0.3$  nM), mMC3R ( $EC_{50} = 14 \pm 2$  nM), and mMC5R ( $EC_{50} = 8.4 \pm 0.6$  nM). At the mMC4R, compound **1** had antagonist activity ( $pA_2 = 6.1 \pm 0.2$ ) and partial agonist activity ( $EC_{50} = 600 \pm 140$  nM; 43% @ 100  $\mu$ M). Compound **2** has nanomolar potency at the MC1R ( $EC_{50} = 10 \pm 0.3$  nM), mMC3R ( $EC_{50} = 16 \pm 2$  nM), and the mMC5R ( $EC_{50} = 8.4 \pm 0.6$  nM). Compound **2** has antagonist activity at the mMC4R ( $pA_2 = 6.1 \pm 0.2$ ). Compound **2** is the most selective compound for the mMC3R over the mMC4R due to the fact that it has micromolar potency as an antagonist at the mMC4R and no measurable mMC4R agonist activity. While compounds **1** and **2** have similar activity profiles and are at least 5-fold more potent at the mMC3R than other substitutions, there do not share many physical properties with the control compound, Ac-His-Arg-(p-I)DPhe-Tic-NH<sub>2</sub>. Both (4,4')DBip (**1**) and the p-tBu (**2**) are both weak electron donating groups, but **1** contains an aromatic substituent and **2** contains an aliphatic substituent. This is dissimilar to the p-I substituent which donates electron density through  $\pi$  bonding, but is electronegative and known to have inductive withdrawal of electrons.

Compounds Ac-His-Arg-DPhe(p-Br)-Tic-NH<sub>2</sub> (**3**), Ac-His-Arg-DPhe(p-Cl)-Tic-NH<sub>2</sub> (**6**), Ac-His-Arg-DPhe-(3,4)diCl-Tic-NH<sub>2</sub> (**7**), and Ac-His-Arg-DPhe(p-F)-Tic-NH<sub>2</sub> (**8**) contained halogens and were chosen to explore trends in lipophilicity and electronegativity. Compound **3** has agonist activity at the MC1R ( $EC_{50} = 0.8 \pm 0.3$  nM), mMC3R ( $EC_{50} = 85 \pm 20$  nM), and the mMC5R ( $EC_{50} = 9.7 \pm 0.5$  nM), while having partial agonist activity at the mMC4R ( $230 \pm 40$  nM; 54% @ 100  $\mu$ M). Compound **3** was of special interest because it has measurable partial agonist activity at the mMC4R but no measurable antagonist activity at the mMC4R. Compound **6** has agonist activity

at the MC1R ( $EC_{50} = 0.95 \pm 0.08$  nM), mMC3R ( $EC_{50} = 140 \pm 20$  nM), and the mMC5R ( $EC_{50} = 19 \pm 6$  nM). Compound **6** had partial agonist activity at the mMC4R ( $380 \pm 50$  nm; 67% @ 100  $\mu$ M). Compound **7** has agonist activity at mMC1R ( $EC_{50} = 0.52 \pm 0.03$  nM), mMC3R ( $EC_{50} = 140 \pm 70$  nM), and mMC5R ( $EC_{50} = 70 \pm 6$  nM). Antagonist activity at the mMC4R ( $pA_2 = 6.23 \pm 0.06$ ) was reported for compound **7**. Agonist activity at the MC1R ( $EC_{50} = 2.2 \pm 0.7$  nM), mMC3R ( $EC_{50} = 450 \pm 70$  nM), and the mMC5R ( $EC_{50} = 5 \pm 4$  nM) was seen when testing compound **8**. Compound **8** had partial agonist activity at the mMC4R ( $560 \pm 60$  nm; 69% @ 100  $\mu$ M). The most efficacious partial agonists were in the halogen series, specifically the compounds **6** (p-F substitution) and **8** (p-Cl substitution).

Trends in the halogen series were explored for mMC3R and mMC4R activity. The less electronegative para position substitutions of iodine and bromine (**3**) were slightly more potent at the mMC3R compared to compounds with more electronegative, smaller halogen substitutions chlorine (**6**) and fluorine (**8**). Antagonist mMC4R activity is only seen in the Ac-His-Arg-DPhe(p-I)-Tic-NH<sub>2</sub>. The partial agonist activity is greater when compounds are substituted at the para position with chlorine and fluorine when compared to bromine and iodine (Table 2).

In order to confirm any trends in electronegativity and lipophilicity found in the halogen series, activity of the p-CF<sub>3</sub> substituted peptide (**4**) was compared with the p-CH<sub>3</sub> substituted peptide (**5**). There was no significant difference between activity at any of the melanocortin receptors tested, except for the partial agonist activity associated with compound **5**. Compound **4** has agonist activity at the MC1R ( $EC_{50} = 6 \pm 2$  nM), mMC3R ( $EC_{50} = 90 \pm 30$  nM), and the mMC5R ( $EC_{50} = 13 \pm 4$  nM), while having antagonist activity at the mMC4R ( $pA_2 = 6.4 \pm 0.2$ ). Compound **5** has agonist activity at the MC1R ( $EC_{50} = 1.2 \pm 0.3$  nM), mMC3R ( $EC_{50} = 110 \pm 20$  nM), and the mMC5R ( $EC_{50} = 14 \pm 4$  nM), while having antagonist activity ( $pA_2 = 6.3 \pm 0.2$ ) and partial agonist activity ( $390 \pm 90$  nm; 67% @ 100  $\mu$ M) at the mMC4R.

Two compounds had micromolar activity at the mMC3R, Ac-His-Arg-DPhe(p-CN)-Tic-NH<sub>2</sub> (**9**), and Ac-His-Arg-DTyr-Tic-NH<sub>2</sub> (**10**). Compound **9** showed agonist activity at the MC1R

( $EC_{50} = 32 \pm 3$  nM), mMC3R ( $EC_{50} = 4000 \pm 1000$  nM), and the mMC5R ( $EC_{50} = 500 \pm 200$  nM). Some agonist activity at the mMC4R was detected ( $EC_{50} = 29\%$  @  $100 \mu\text{M}$ ) when testing compound **9**. Compound **10** showed agonist activity at the MC1R ( $EC_{50} = 50 \pm 10$  nM), mMC3R ( $EC_{50} = 4300 \pm 800$  nM), and the mMC5R ( $EC_{50} = 1200 \pm 600$  nM). The polar groups (OH) in DTyr (compound **10**) and (p-CN) in compound **9** decrease the ability of the compounds to activate the MC1R, MC3R and MC5R by greater than 100 fold compared to Ac-His-Arg-DPhe(p-I)-Tic-NH<sub>2</sub>. Compound **9** and **10** lose antagonist activity compared to the low nanomolar mMC3R compounds (Table 2).

The main goal of this study was to develop a probe that minimizes mMC4R activity in order to study mMC3R activity thoroughly. Before the positional scan for MC3R selective compounds that developed possible mMC3R selective compounds<sup>38</sup>, analogs of endogenous ligands  $\gamma_2$ -MSH and  $\alpha$ -MSH were studied. By increasing the selectivity of the Ac-His-Arg-DPhe(p-I)-Tic-NH<sub>2</sub> scaffold for the mMC3R over the mMC4R, we are developing compounds that have more drug-like properties than previous endogenous analogs. These compounds could be tested *in vivo* as therapies for obesity possibly without creating undesirable side effects of previous melanocortin therapeutics primarily targeting the MC4R.

## **Discussion**

A structure-activity relationship study was conducted by substituting (p-I)DPhe residues with a series of aromatic amino acids in the tetrapeptide scaffold Ac-His-Arg-(p-I)DPhe-Tic-NH<sub>2</sub>. This scaffold was originally investigated for its unique pharmacological profile and the fact that it contained a 'Arg-(p-I)DPhe' motif which reversed the positions of the traditional agonist 'Phe-Arg' motif seen in the endogenous agonist sequence His-Phe-Arg-Trp<sup>18</sup>. It was hypothesized that the (pI)DPhe position in Ac-His-Arg-(pI)DPhe-Tic-NH<sub>2</sub> could be important to increasing agonist activity selective for the mMC3R receptor when compared with mMC4R. A series of mono- and di- substituted DPhe substituents were chosen to explore the physicochemical properties that contribute to selectivity of the mMC3R over the mMC4R. The tetrapeptides were characterized *in*

*vitro* using the stably transfected mouse MC1R, MC3R, MC4R, and MC5R in HEK293 cells (Table 2, 3).

#### *Polar Group Substitutions*

Two polar groups were incorporated into the SAR, tetrapeptide **9** and **10** which substituted (p-CN)DPhe and DTy into the tetrapeptide scaffold, respectively. Both peptides have similar pharmacological profiles at all receptors that were studied. Tetrapeptides **9** and **10** both saw 100-fold decreased potency at the mMC3R, mMC4R, and mMC5R when compared to the Ac-His-Arg-DPhe(p-I)-Tic-NH<sub>2</sub> control (Figure 2C). Potency at the MC1R also decreased when compared to the controls, by 40 to 63-fold, however both compound **9** and **10** were about 15-fold more potent at the mMC1R than at any other receptor. This could suggest that the polar groups are not well tolerated by the MC3R, MC4R or MC5R and that the DPhe structures are interacting with a hydrophobic pocket. Through homology modeling and mutation studies the DPhe substituent in the DPhe-Arg-Trp melanocortin agonist sequence and the Arg-Phe-Phe antagonist sequence are both predicted to interact with aromatic residues in the mMC4R binding domain<sup>52-54</sup>. It was also hypothesized previously that Ac-His-Arg-DPhe-Tic-NH<sub>2</sub> scaffold's mixed pharmacology is caused by the scaffold being a hybrid between the tripeptide AgRP sequence, "Arg-Phe-Phe" and the melanocortin agonist signal sequence "His-Phe-Arg-Trp"<sup>37</sup>. It could be possible that this group of tetrapeptides also binds in the same pocket, and hence more polar hydrophilic groups would have less activity.

#### *Hydrophobic Substitutions*

Hydrophobic groups such as the tetrapeptides with DBip (**1**), p-tBu (**2**) and p-Me (**5**) substitutions, experienced a range of mMC3R EC<sub>50</sub> values (13 nM < EC<sub>50</sub> < 110 nM) (Figure 2B). The bulkier groups of compound **1** and **2** are 8-fold more potent at the mMC3R compared to compound **5**. The most potent mMC3R hydrophobic substitutions are sterically bulky. Compounds **1** and **2**, containing substitutions DBip, and p-tBu, respectively, are 6.8-fold more potent at the mMC3R compared to the p-Me substitution. At the mMC4R all of the compounds possessing

hydrophobic substitutions were antagonists, mMC4R antagonism potency tends to increase when agonist potency at mMC3R increases. All hydrophobic groups except compound **2** show partial agonist activity at the mMC4R (Figure 3B).

#### *Electrostatics*

The electrostatics of the tetrapeptides were studied due to trends seen in halogen data series<sup>51</sup>. Computational modeling for a similar tetrapeptide SAR has previously allowed for the study between biophysical properties and ligand-receptor interactions by modeling data from a halogen series<sup>51</sup>. In Figure 6, it can be seen that the compounds that had the lowest potency at the mMC3R (Figure 6B) quite consistently have a larger build-up of negative charge at the DPhe substituent than the higher potency agonists at the mMC3R (Figure 6A). Each of the compounds in Figure 6B, **8** (p-F), **9** (p-CN), and **10** (p-OH), have an electronegative atom which is surrounded by many more electropositive atoms, this creates a dipole giving a partial negative charge on the surface of the molecules. This dipole effect is muted in other tetrapeptides due to numerous factors such as reduced electronegativity and increased symmetry between dipoles in the substituents of the other tetrapeptides. Less electronegative substitutions, such as the p-I, p-tBu, and DBip, were greater than 28-fold more potent at the mMC3R as compared to the para-fluoro substitution. Compound **4** has a p-CF<sub>3</sub> substituent and is 5-fold more potent than the p-F containing compound. While fluorine is extremely electronegative, the fluorine atoms in compound **4** are organized around the carbon in a symmetrical fashion canceling out each of their individual dipoles. However, the electrostatic interactions in the low nanomolar potency mMC3R agonists varies, therefore electrostatics is not sufficient to fully explain the trends seen in mMC3R potency.

#### *Halogen Substitutions: Electronegativity and Lipophilicity*

The electrostatic results match the trends seen in the halogen series, which show that the more electronegative the halogen, the lower the potency at the mMC3R. The trend in electronegativity is as follows: F > 3,4-diCl > Cl > Br > I. Potency in the mMC3R is the reverse of

the electronegativity trend, where the p-I ligand is the most potent halogen and the p-F compound is the least potent halogen (Figure 2). The antagonist activity at the mMC4R is only seen in the control ligand and the (3,4)-diCl compound (Figure 4 and 5). Both mMC3R and mMC4R activity seem to rely on electronegativity. However, there is also no statistical difference between the mMC3R agonist or mMC4R antagonist activity of the compound with a p-CF<sub>3</sub> (**4**) substitution and the compound with a p-CH<sub>3</sub> (**5**) substitution. This shows that electronegativity is not the only factor influencing the trends seen in mMC3R or mMC4R antagonist activity.

One of the other trends that was explored was that of lipophilicity. Lipophilicity increases as follows: F < Cl < Br < CF<sub>3</sub> < I < 3,4-diCl. The potency at the mMC3R data weakly supports a trend in lipophilicity: a more lipophilic substitution resulted in higher potency at the mMC3R (Table 2). However, the (3,4)-diCl containing compound (**7**) is not as potent as the control tetrapeptide containing p-I. There is a non-significant trend seen that logP<sub>oct/water</sub> was more negative as potency at the mMC3R went down (Figure 7). LogP<sub>oct/water</sub> values were calculated as QPLogP<sub>oct/water</sub> values using Maestro QikProp tool (Table 4).

### *Selectivity*

The SAR presented created more selective tetrapeptides over the mMC4R that eliminated much of the mMC4R agonist and antagonist activity in previous tetrapeptides while keeping low nanomolar potency at the mMC3R. Three new compounds containing: (3,4)-diCl, DBip, and p-tBu, were found to be equipotent at the mMC1R, mMC3R and mMC5R compared to Ac-His-Arg-(pI)DPhe-Tic-NH<sub>2</sub>. Compound **2** (p-tBu) was of interest because it is the most selective for the mMC3R over the mMC4R. This compound showed no notable agonist activity at the mMC4R and the mMC4R antagonist activity is at micromolar affinity compared to the low nanomolar agonist potency at the mMC3R. In general, as a compound becomes more potent at the mMC3R it also becomes a more potent antagonist at the mMC4R (Table 2). For this reason, compound **3** (p-Br) was of interest because it still contains nanomolar potency at the mMC3R but it has no measurable antagonist mMC4R activity.

The DPhe substituent correlates with mMC4R agonist activity as seen by lipophilicity trends in the halogen series, however it is likely that there are other factors influencing mMC4R activity that have not been covered in this study. In order to study trends in mMC4R activity more thoroughly, SAR at the Arg position of the His-Arg-(pI)DPhe-Tic compound could be completed.

While trends in mMC4R agonist activity and antagonist activity were not significant in this study, the DPhe substituent contributes to mMC3R activity as seen by trends in steric interactions, lipophilicity and electrostatics. The mMC3R nanomolar agonist and mMC4R partial agonist/antagonist pharmacological profile is unique to the scaffold His-Arg-DPhe-Tic, explored in the TaMALES library. The His-Arg-DPhe-Tic scaffold reverses the order of the DPhe and Arg residues found in the common melanocortin agonist scaffold: His-DPhe-Arg-Trp. When the DPhe position of the His-DPhe-Arg-Trp scaffold was explored through SAR, compounds with mMC4R agonist activity and mMC3R partial agonist/antagonist activity were found<sup>51</sup>. This evidence supports the importance of the position of the DPhe residue in the His-Arg-DPhe-Tic scaffold for mMC3R selectivity over the mMC4R.

## **Conclusions**

The SAR presented created a more selective tetrapeptides that eliminated much of the mMC4R agonist and antagonist activity while keeping low nanomolar potency at the mMC3R. The compounds are not truly selective for mMC3R due to their activity at the mMC1R and mMC5R. We propose that a combination of electrostatic properties, lipophilicity and steric factors contribute to making more potent mMC3R agonists. These compounds can be used to further investigate the physiological role of the MC3R and determine if it is a worthwhile drug target for treating metabolic diseases.

**Table 1. Tetrapeptide Characterization<sup>a</sup>**

Compound	Sequence	Observed Mass [M+1] (g/mol)	Calculated Exact Mass (g/mol)	Purity (%)	Retention Time in Acetonitrile (min)	Retention Time in Methanol (min)
-	Ac-His-DPhe-Arg-Trp-NH <sub>2</sub>	686.4	685.3	> 98	10.11	15.60
-	Ac-His-Arg-DPhe(p-I)-Tic-NH <sub>2</sub>	785.3	784.2	> 98	14.89	21.77
<b>1</b>	Ac-His-Arg-(4,4')DBip-Tic-NH <sub>2</sub>	735.5	734.3	> 96	16.66	25.89
<b>2</b>	Ac-His-Arg-DPhe(p-tBu)-Tic-NH <sub>2</sub>	715.4	714.4	> 95	17.46	27.04
<b>3</b>	Ac-His-Arg-DPhe(p-Br)-Tic-NH <sub>2</sub>	737.3, 739.3	736.3, 738.3	> 97	14.89	26.07
<b>4</b>	Ac-His-Arg-DPhe(p-CF <sub>3</sub> )-Tic-NH <sub>2</sub>	727.5	726.7	> 97	15.00	23.38
<b>5</b>	Ac-His-Arg-DPhe(p-Me)-Tic-NH <sub>2</sub>	673.5	672.4	> 98	14.31	22.34
<b>6</b>	Ac-His-Arg-DPhe(p-Cl)-Tic-NH <sub>2</sub>	693.5	692.3	> 98	14.61	22.70
<b>7</b>	Ac-His-Arg-(3,4-diCl)DPhe-Tic-NH <sub>2</sub>	727.4	726.3	> 98	15.60	23.98
<b>8</b>	Ac-His-Arg-DPhe(p-F)-Tic-NH <sub>2</sub>	677.5	676.3	> 95	13.55	20.82
<b>9</b>	Ac-His-Arg-DPhe(p-CN)-Tic-NH <sub>2</sub>	684.3	683.3	> 98	11.50	17.25
<b>10</b>	Ac-His-Arg-DTyr-Tic-NH <sub>2</sub>	675.4	674.3	> 97	10.49	15.03

<sup>a</sup>The pure compounds were characterized analytically using RP-HPLC with two solvent systems. Both acetonitrile and methanol 10-90% gradients were run in 0.1% TFA in water for 35 min. By integrating the area under the curve at 214 nm purity was determined for each compound. The mass was confirmed using ESI/TOF-MS

**Table 2. Agonist and Antagonist Activity of DPhe Substitutions at the mMC3R, mMC4R and mMC5R<sup>a</sup>**

#	Sequence	mMC3R Agonist EC <sub>50</sub> ± SEM (nM)	Fold	mMC4R		mMC5R Agonist EC <sub>50</sub> ± SEM (nM)
				Agonist EC <sub>50</sub> ± SEM (nM)	Antagonist pA <sub>2</sub> ± SEM	
<b>NDP-MSH</b>	Ac-Ser-Tyr-Ser-Nle-Glu-His-DPhe-Arg-Trp-Lys-Pro-Val-NH <sub>2</sub>	0.42 ± 0.02	-	0.32 ± 0.03	-	0.9 ± 0.2
-	Ac-His-DPhe-Arg-Trp-NH <sub>2</sub>	190 ± 40	-	12 ± 3	-	4.3 ± 2
-	Ac-His-Arg-DPhe-Trp-NH <sub>2</sub>	1300 ± 300	-	3000 ± 1000	-	150 ± 60
-	Ac-His-Arg-DPhe(p-I)-Tic-NH <sub>2</sub>	13 ± 2	1.0	70 ± 13 (32%)	7.2 ± 0.7	4.5 ± 1
<b>1</b>	Ac-His-Arg-(4,4')DBip-Tic-NH <sub>2</sub>	14 ± 2	1.1	600 ± 140 (43%)	6.1 ± 0.2	8.4 ± 0.6
<b>2</b>	Ac-His-Arg-DPhe(p-tBu)-Tic-NH <sub>2</sub>	16 ± 2	1.2	> 100 μM	6.8 ± 0.3	3.3 ± 0.6
<b>3</b>	Ac-His-Arg-DPhe(p-Br)-Tic-NH <sub>2</sub>	85 ± 20	6.5	230 ± 40 (54%)	N/A	9.7 ± 0.5
<b>4</b>	Ac-His-Arg-DPhe(p-CF <sub>3</sub> )-Tic-NH <sub>2</sub>	90 ± 30	6.9	> 100 μM	6.4 ± 0.2	13 ± 4
<b>5</b>	Ac-His-Arg-DPhe(p-Me)-Tic-NH <sub>2</sub>	110 ± 20	8.5	390 ± 90 (46%)	6.3 ± 0.2	14 ± 4
<b>6</b>	Ac-His-Arg-DPhe(p-Cl)-Tic-NH <sub>2</sub>	140 ± 20	11	380 ± 50 (63%)	N/A	19 ± 6
<b>7</b>	Ac-His-Arg-(3,4-diCl)DPhe-Tic-NH <sub>2</sub>	250 ± 40	19	> 100 μM	6.23 ± 0.06	70 ± 6
<b>8</b>	Ac-His-Arg-DPhe(p-F)-Tic-NH <sub>2</sub>	450 ± 70	35	560 ± 60 (69%)	N/A	5 ± 4
<b>9</b>	Ac-His-Arg-DPhe(p-CN)-Tic-NH <sub>2</sub>	4000 ± 1000	308	29% @ 100 μM	N/A	500 ± 200
<b>10</b>	Ac-His-Arg-DTyr-Tic-NH <sub>2</sub>	4300 ± 800	331	> 100 μM	N/A	1200 ± 600

---

<sup>a</sup>Data summary from colorimetric assay that gives a signal proportional to increases in cAMP. Data was collected from three independently conducted experiments, each with duplicate replicates. NDP-MSH, Ac-His-DPhe-Arg-Trp-NH<sub>2</sub> and forskolin were all used as positive controls. Adenylate cyclase is activated by forskolin independently of the melanocortin system. Assay media was used as a negative control. Activity for partial agonists is recorded as an EC<sub>50</sub> value followed by the percentage of NDP-MSH maximum activation of the receptor at 100 μM in parenthesis. Activity for less than full agonists is denoted as a percentage of NDP-MSH maximal activation of the receptor. Compounds with less than 20% activity compared to maximal percent activation of NDP-MSH are recorded as EC<sub>50</sub> > 100000 nM. Antagonist activity was tested using NDP-MSH as an agonist and ligand concentrations of: 10000, 5000, 1000, and 500nM. Dose dependent shifts in EC<sub>50</sub> enables the calculation of a pA<sub>2</sub> value determined by Schild analysis<sup>55</sup>. If no shift is detected in the antagonist experiment, the outcome is denoted by “N/A” meaning there is no activity observed up to 10uM. Fold values were calculated in comparison to the mMC3R potency of c-His-Arg-DPhe(p-I)-Tic-NH<sub>2</sub>.

**Table 3. Agonist Activity of DPhe Substitutions at the mMC1R<sup>a</sup>**

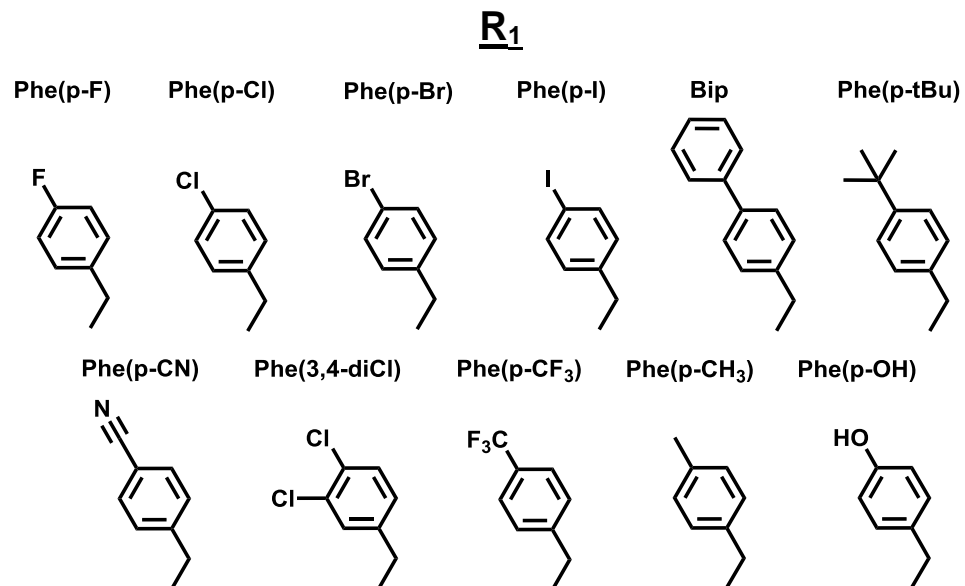
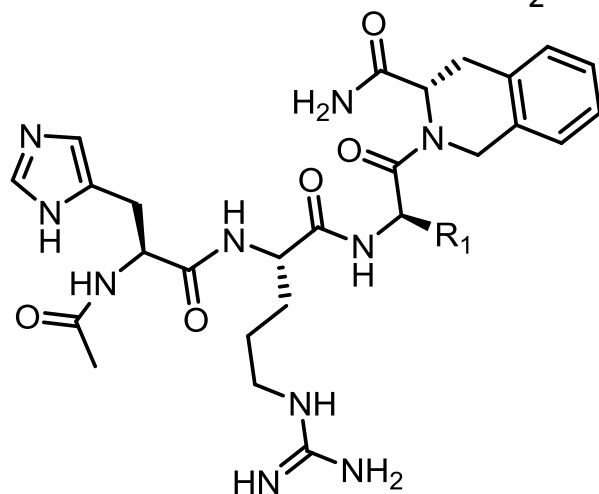
<b>Compound</b>	<b>Sequence</b>	<b>mMC1R Agonist EC<sub>50</sub> + SEM (nM)</b>
NDP-MSH	Ac-Ser-Tyr-Ser-Nle-Glu-His-DPhe-Arg-Trp-Lys-Pro-Val-NH <sub>2</sub>	0.012 ± 0.002
-	Ac-His-DPhe-Arg-Trp-NH <sub>2</sub>	10 ± 4
-	Ac-His-Arg-DPhe(p-I)-Tic-NH <sub>2</sub>	0.8 ± 0.3
<b>1</b>	Ac-His-Arg-(4,4')DBip-Tic-NH <sub>2</sub>	0.52 ± 0.03
<b>2</b>	Ac-His-Arg-DPhe(p-tBu)-Tic-NH <sub>2</sub>	10 ± 3
<b>3</b>	Ac-His-Arg-DPhe(p-Br)-Tic-NH <sub>2</sub>	0.8 ± 0.3
<b>4</b>	Ac-His-Arg-DPhe(p-CF <sub>3</sub> )-Tic-NH <sub>2</sub>	6 ± 2
<b>5</b>	Ac-His-Arg-DPhe(p-Me)-Tic-NH <sub>2</sub>	1.2 ± 0.3
<b>6</b>	Ac-His-Arg-DPhe(p-Cl)-Tic-NH <sub>2</sub>	0.95 ± 0.08
<b>7</b>	Ac-His-Arg-(3,4-diCl)DPhe-Tic-NH <sub>2</sub>	6 ± 2
<b>8</b>	Ac-His-Arg-DPhe(p-F)-Tic-NH <sub>2</sub>	2.2 ± 0.7
<b>9</b>	Ac-His-Arg-DPhe(p-CN)-Tic-NH <sub>2</sub>	32 ± 3
<b>10</b>	Ac-His-Arg-DTyr-Tic-NH <sub>2</sub>	50 ± 10

<sup>a</sup>Data summary from intracellular cAMP readings using AlphaScreen (PerkinElmer). Data was collected from three independently conducted experiments, each with duplicate replicates. NDP-MSH, Ac-His-DPhe-Arg-Trp-NH<sub>2</sub> and forskolin were all used as positive controls. Adenylate cyclase is activated by forskolin independently of the melanocortin system. Assay media was used as a negative control.

**Table 4.** Calculated Properties of Tetrapeptides

Entry ID	Substitution	MC3R Agonist Activity (EC <sub>50</sub> nM)	Potential Energy-OPLS- 2005 (KJ/mol)	Hydrogen Bond Donors	Hydrogen Bond Acceptors	Polarizability (Å <sup>3</sup> )	logP <sub>o/w</sub>	Polar Surface Area (Å <sup>2</sup> )
KNS2224	pI	13	-862	7.75	14.25	64	-0.399	266
KNS2231	DBip	14	-875	7.75	14.25	69	0.505	253
KNS2233	ptBu	16	-924	7.75	14.25	72	0.665	267
KNS2223	pBr	85	-856	7.75	14.25	62	-0.223	252
KNS2236	pCF <sub>3</sub>	90	-866	7.75	14.25	64	-0.649	266
KNS2237	pCH <sub>3</sub>	110	-872	7.75	14.25	70	-0.355	269
KNS2221	pCl	140	-776	7.75	14.25	68	0.019	269
KNS2234	(3,4,)diCl	250	-829	7.75	14.25	67	-0.121	270
KNS2222	pF	450	-778	7.75	14.25	67	-0.205	273
KNS2238	pCN	4000	-872	7.75	15.75	65	-1.034	290
KNS2239	pOH	4300	-893	8.75	15	67	-1.235	291

Ac-His-Arg-XXX-Tic-NH<sub>2</sub>



Tetrapeptide Melanocortin Agonist  
Ligands to Explore Selectivity  
(TaMALES) Library

Figure 1. TaMALES library scaffold and the amino acid side chains used in the peptide library.

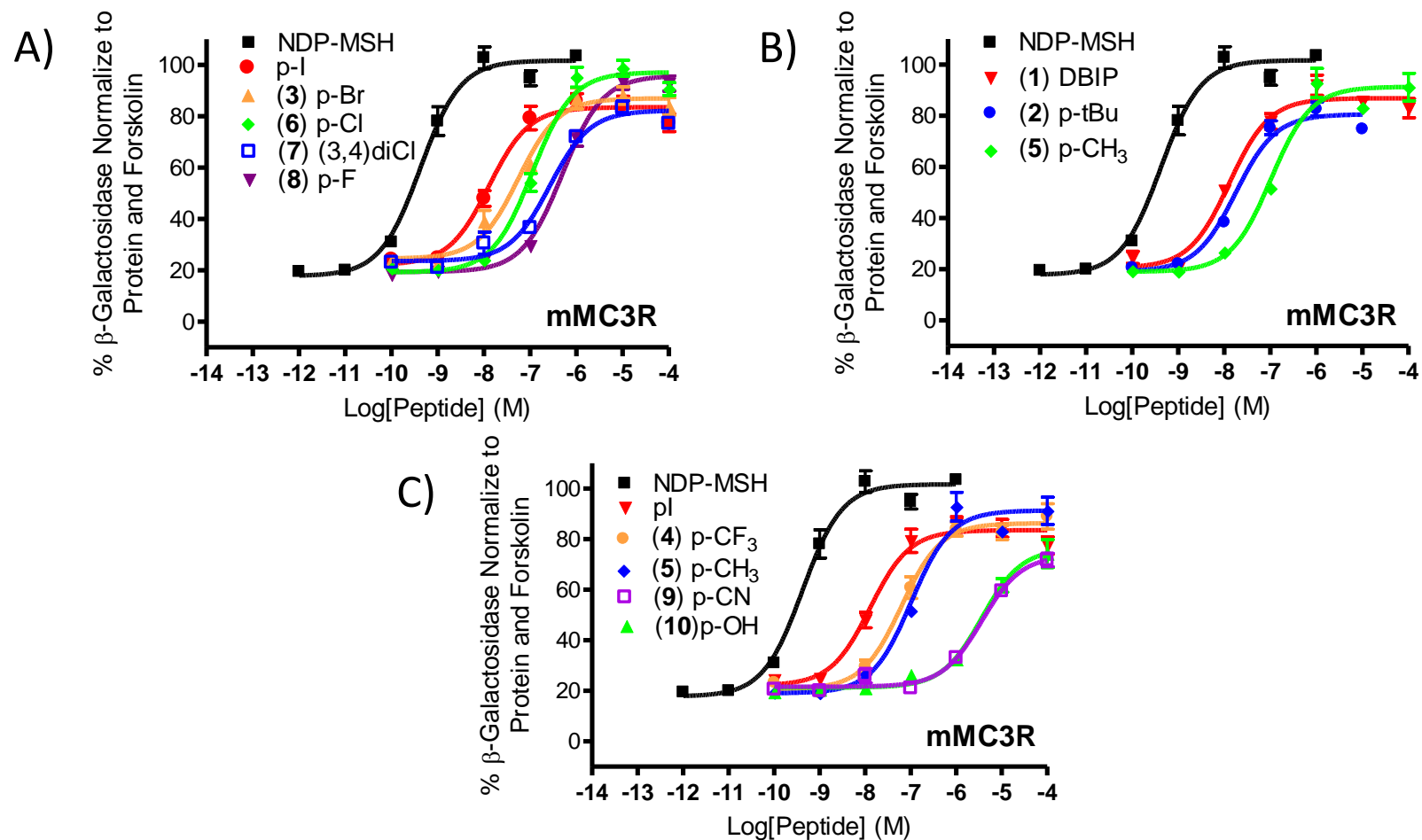


Figure 2. Illustration of agonist activity observed mouse melanocortin-3 receptor. A) Halogen series of substitutions with the Ac-His-Arg-(pI)DPhe-Tic-NH<sub>2</sub> control annotated as p-I. B) Hydrophobic series of substitutions. C) The Ac-His-Arg-(pI)DPhe-Tic-NH<sub>2</sub> control annotated as pI, the methyl substituent, p-CF<sub>3</sub> substituent, and the two substituents with micromolar potency (p-CN and p-OH substituent).

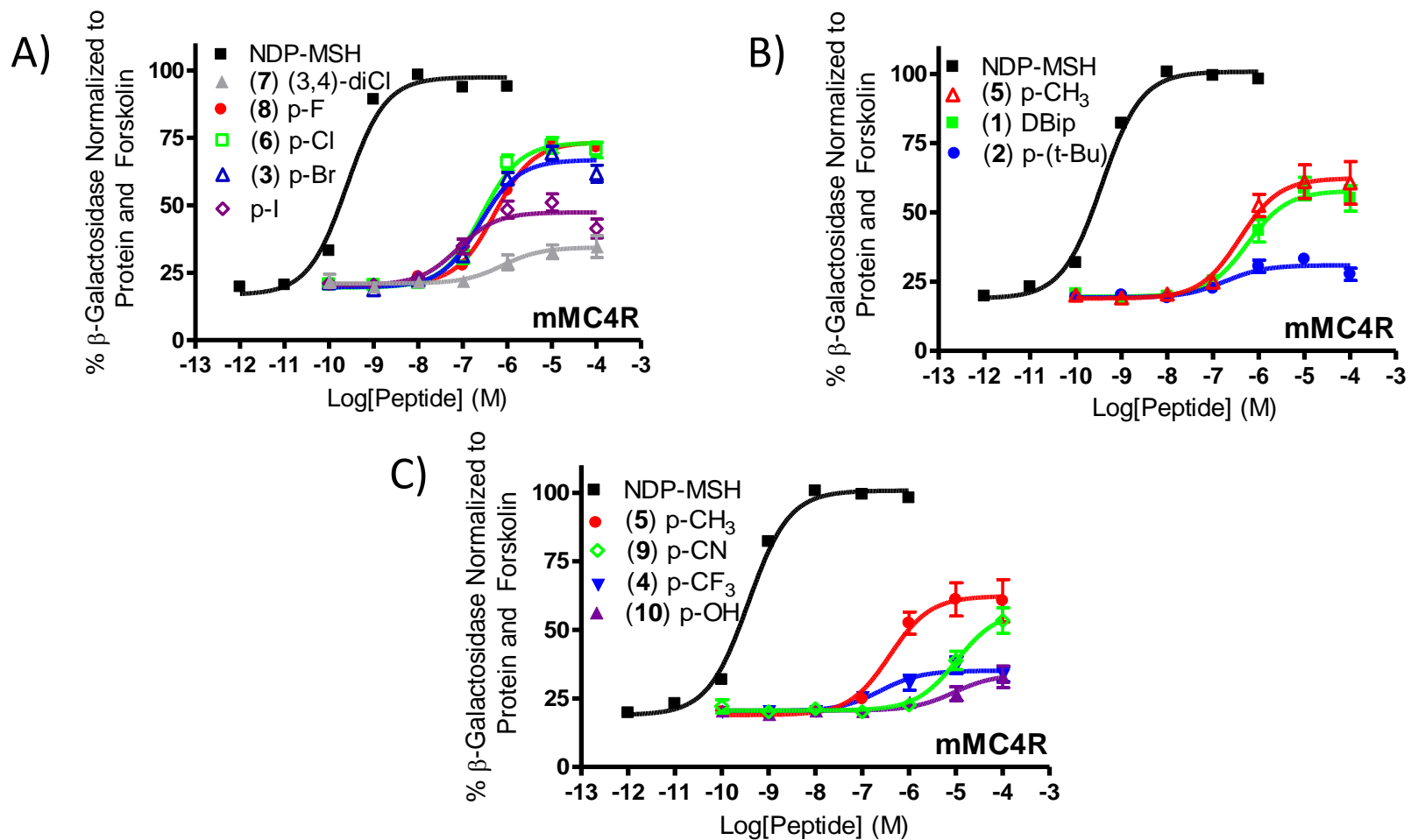


Figure 3. Illustration of agonist activity observed mouse melanocortin-4 receptor. A) Halogen series of substitutions with the Ac-His-Arg-(pI)DPhe-Tic-NH<sub>2</sub> control annotated as p-I. B) Hydrophobic series of substitutions. C) The methyl substituent, p-CF<sub>3</sub> substituent, and the two substituents with micromolar potency (p-CN and p-OH substituents).

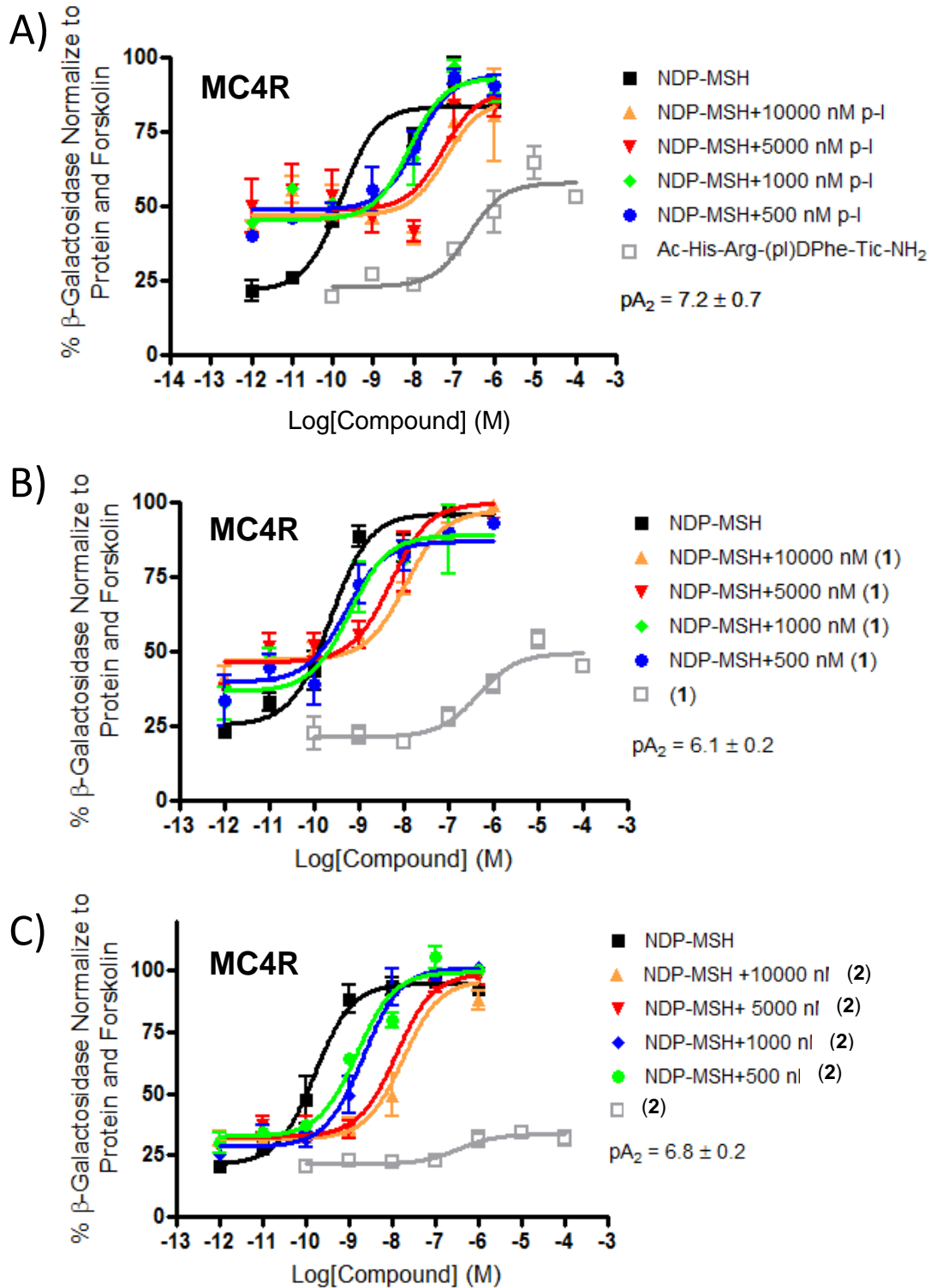


Figure 4. Illustration of antagonist activity observed at the mouse melanocortin-4 receptor from the most potent-MC3R agonists. A) Illustration of mMC4R antagonist data from the control peptide: Ac-His-Arg-(pI)DPhe-Tic-NH<sub>2</sub>. B) Depiction of mMC4R antagonist data from Ac-His-Arg-DBip-Tic-NH<sub>2</sub>. C) Depiction of mMC4R antagonist data from Ac-His-Arg-(p-tBu)DPhe-Tic-NH<sub>2</sub>. The  $pA_2$  values are calculated using Schild analysis. The  $pA_2 = -\text{Log}(K_i)$ .

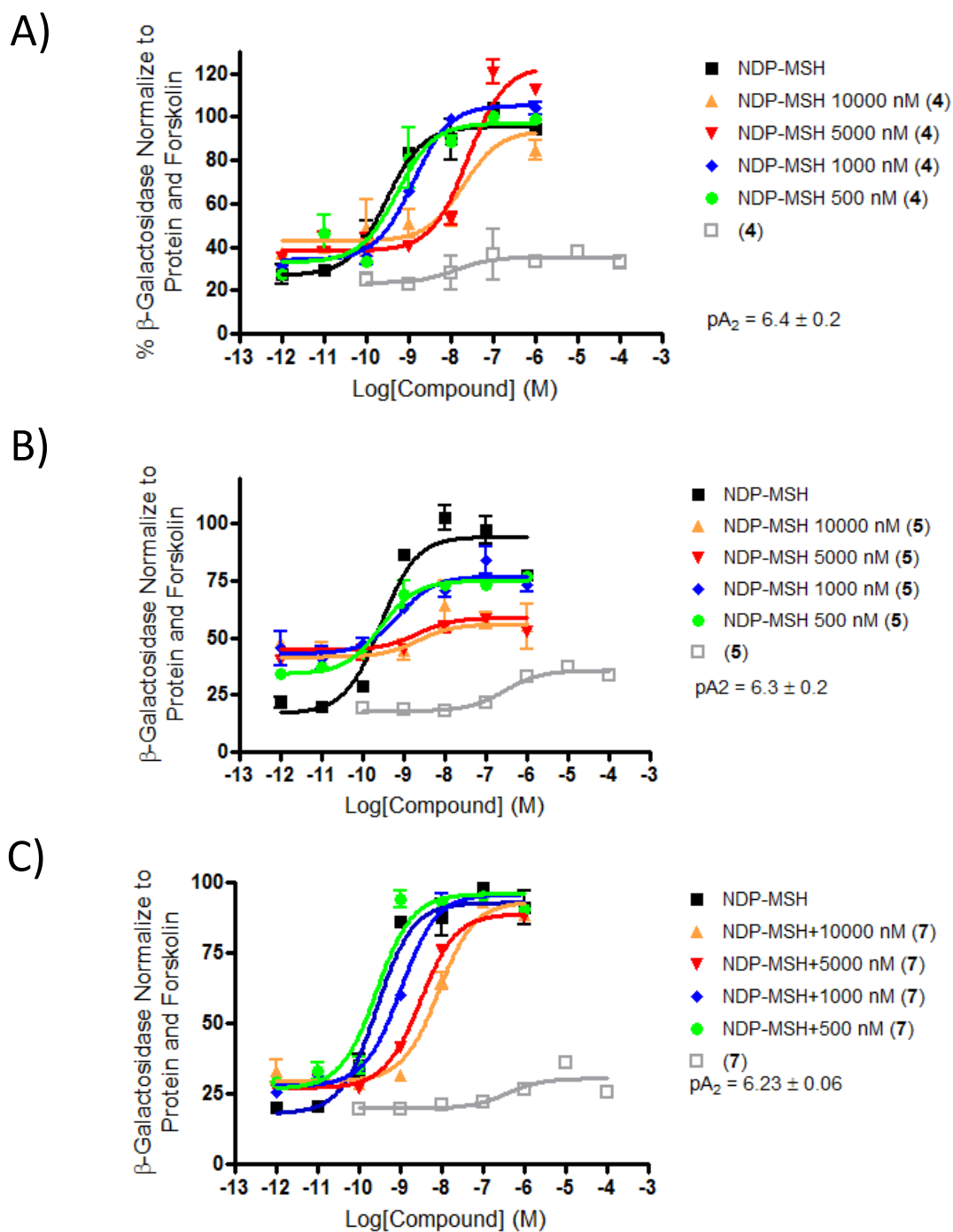


Figure 5. Illustration of antagonist activity observed at the mouse melanocortin-4 receptor. A) Illustration of mMC4R antagonist data from the control peptide: Ac-His-Arg-(pCF<sub>3</sub>)DPhe-Tic-NH<sub>2</sub>. B) Depiction of mMC4R antagonist data from Ac-His-Arg-(pCH<sub>3</sub>)DPhe-Tic-NH<sub>2</sub>. C) Depiction of mMC4R antagonist data from Ac-His-Arg-(3,4)-diCl)DPhe-Tic-NH<sub>2</sub>. The pA<sub>2</sub> values are calculated using Schild analysis. The pA<sub>2</sub> = -Log(K<sub>i</sub>).

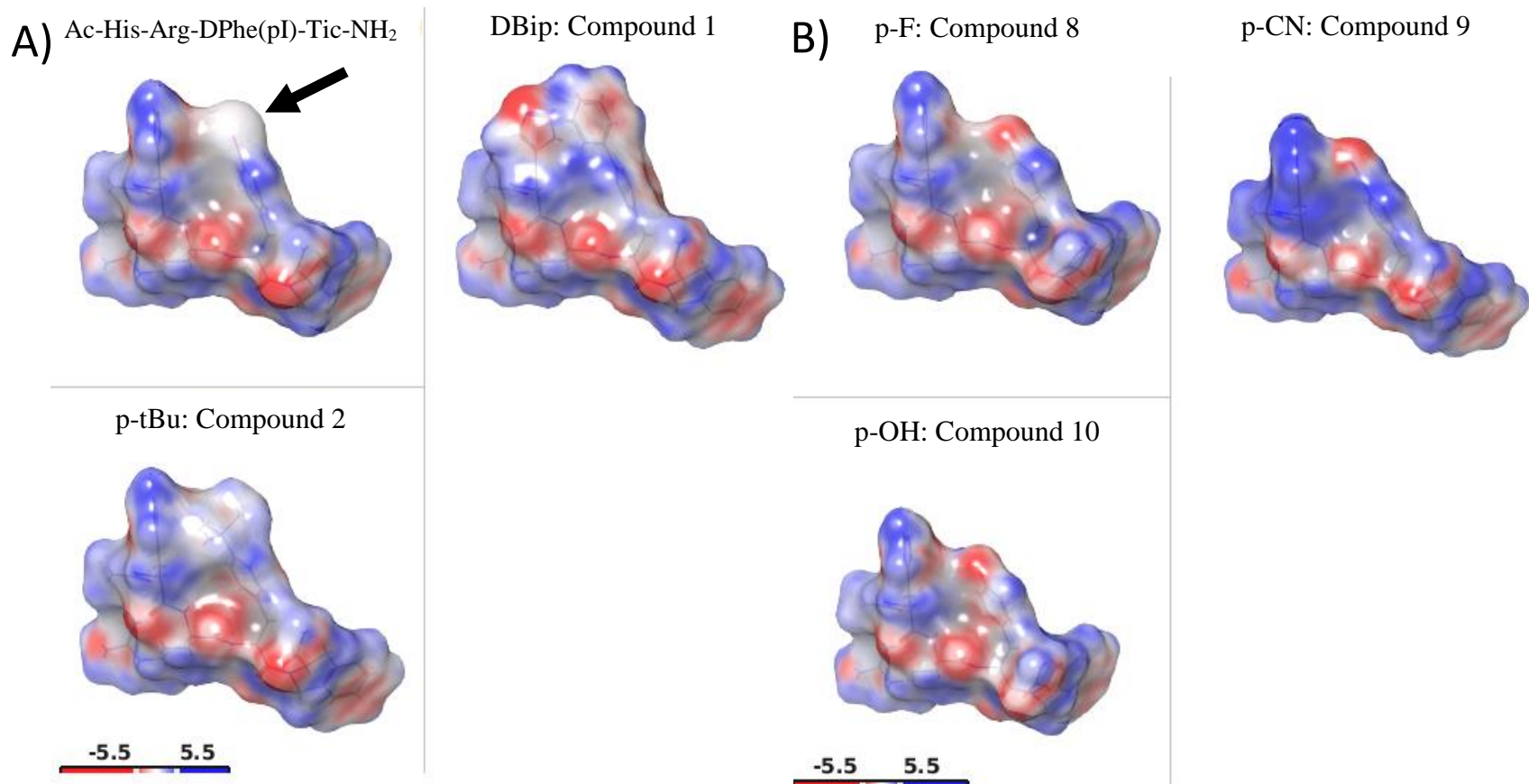


Figure 6. Electrostatic potentials calculated with Maestro. Red represents electronegative (-5.5 kT/e), blue represents electropositive (+5.5 kT/e). The molecule is oriented with the histidine residue facing upwards on the left hand side, the arginine is in the bottom left corner, the DPhenylalanine substitutions are facing upward on the right hand side and the Tic residue is in the bottom right corner. The DPhenylalanine substitution is circled in black on the first compound. **A)** Low nanomolar potency mMC3R compounds including: compound **1**, **2** and the control para iodo compound. **B)** Micromolar potency mMC3R compounds including: compound **8**, **9**, and **10**.

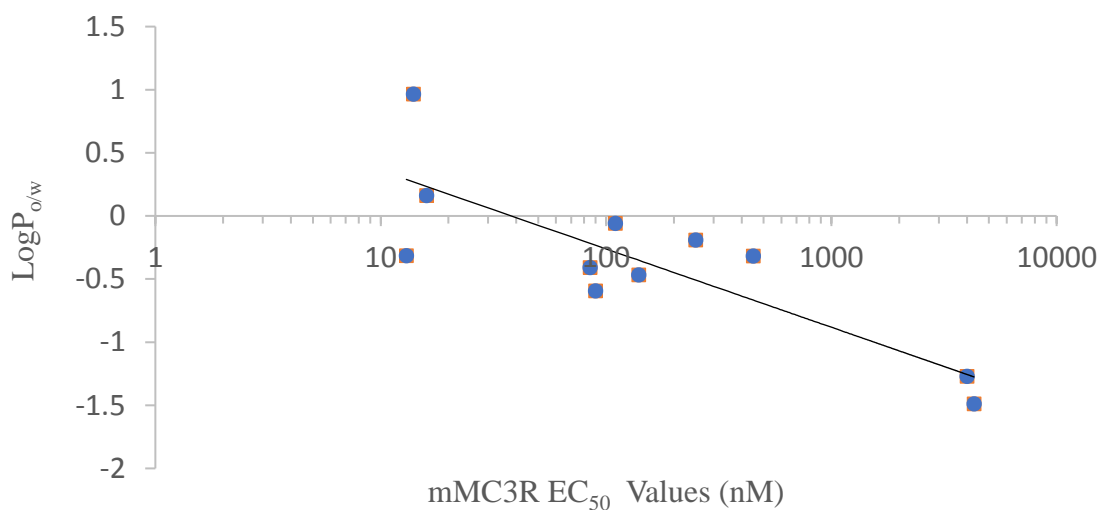


Figure 7. A scatterplot showing the potential trend between partition coefficient of octenol over water and mMC3R EC<sub>50</sub> values. The x-axis is on a logarithmic scale. LogP<sub>o/w</sub> values were calculated in Maestro. There is a slight trend when logP<sub>o/w</sub> values go down the EC<sub>50</sub> also decreases. The trend is not statistically significant, when it is fit with logarithmic regression line the R<sup>2</sup> value is 0.6866.

## References

1. Mountjoy, K.; Robbins, L.; Mortrud, M.; Cone, R. The cloning of a family of genes that encode the melanocortin receptors. *Science* **1992**, *257*, 1248-1251.
2. Roselli-Reh fuss, L.; Mountjoy, K. G.; Robbins, L. S.; Mortrud, M. T.; Low, M. J.; Tatro, J. B.; Entwistle, M. L.; Simerly, R. B.; Cone, R. D. Identification of a receptor for gamma melanotropin and other proopiomelanocortin peptides in the hypothalamus and limbic system. *Proc Natl Acad Sci U S A* **1993**, *90*, 8856-60.
3. Gantz, I.; Shimoto, Y.; Konda, Y.; Miwa, H.; Dickinson, C. J.; Yamada, T. Molecular cloning, expression, and characterization of a fifth melanocortin receptor. *Biochem Biophys Res Commun* **1994**, *200*, 1214-20.
4. Gantz, I.; Konda, Y.; Tashiro, T.; Shimoto, Y.; Miwa, H.; Munzert, G.; Watson, S. J.; DelValle, J.; Yamada, T. Molecular cloning of a novel melanocortin receptor. *J Biol Chem* **1993**, *268*, 8246-50.
5. Gantz, I.; Miwa, H.; Konda, Y.; Shimoto, Y.; Tashiro, T.; Watson, S. J.; DelValle, J.; Yamada, T. Molecular cloning, expression, and gene localization of a fourth melanocortin receptor. *J Biol Chem* **1993**, *268*, 15174-9.
6. Chhajlani, V.; Wikberg, J. E. S. Molecular cloning and expression of the human melanocyte stimulating hormone receptor cDNA. *FEBS Letters* **1992**, *309*, 417-420.
7. Huszar, D.; Lynch, C. A.; Fairchild-Huntress, V.; Dunmore, J. H.; Fang, Q.; Berkemeier, L. R.; Gu, W.; Kesterson, R. A.; Boston, B. A.; Cone, R. D.; Smith, F. J.; Campfield, L. A.; Burn, P.; Lee, F. Targeted Disruption of the Melanocortin-4 Receptor Results in Obesity in Mice. *Cell* **1997**, *88*, 131-141.
8. Butler, A. A.; Kesterson, R. A.; Khong, K.; Cullen, M. J.; Pelleymounter, M. A.; Dekoning, J.; Baetscher, M.; Cone, R. D. A Unique Metalolic Sysdrone Causes Obesity in the Melanocortin-3 Receptor-Deficient Mouse. *Endocrinology* **2000**, *141*, 3518-3521.
9. Chen, A. S.; Marsh, D. J.; Trumbauer, M. E.; Frazier, E. G.; Guan, X. M.; Yu, H.; Rosenblum, C. I.; Vongs, A.; Feng, Y.; Cao, L.; Metzger, J. M.; Strack, A. M.; Camacho, R. E.; Mellin, T. N.; Nunes, C. N.; Min, W.; Fisher, J.; Gopal-Truter, S.; MacIntyre, D. E.; Chen, H. Y.; Van der Ploeg, L. H. Inactivation of the mouse melanocortin-3 receptor results in increased fat mass and reduced lean body mass. *Nat Genet* **2000**, *26*, 97-102.
10. Fan, W.; Boston, B. A.; Kesterson, R. A.; Hruby, V. J.; Cone, R. D. Role of melanocortinergic neurons in feeding and the agouti obesity syndrome. *Nature* **1997**, *385*, 165.
11. Willer, C. J.; Speliotes, E. K.; Loos, R. J.; Li, S.; Lindgren, C. M.; Heid, I. M.; Berndt, S. I.; Elliott, A. L.; Jackson, A. U.; Lamina, C.; Lettre, G.; Lim, N.; Lyon, H. N.; McCarroll, S. A.; Papadakis, K.; Qi, L.; Randall, J. C.; Roccascocca, R. M.; Sanna, S.; Scheet, P.; Weedon, M. N.; Wheeler, E.; Zhao, J. H.; Jacobs, L. C.; Prokopenko, I.; Soranzo, N.; Tanaka, T.; Timpson, N. J.; Almgren, P.; Bennett, A.; Bergman, R. N.; Bingham, S. A.; Bonnycastle, L. L.; Brown, M.; Burt, N. P.; Chines, P.; Coin, L.; Collins, F. S.; Connell, J. M.; Cooper, C.; Smith, G. D.; Dennison, E. M.; Deodhar, P.; Elliott, P.; Erdos, M. R.; Estrada, K.; Evans, D. M.; Gianniny, L.; Gieger, C.; Gillson, C. J.; Guiducci, C.; Hackett, R.; Hadley, D.; Hall, A. S.; Havulinna, A. S.; Hebebrand, J.; Hofman, A.; Isomaa, B.; Jacobs, K. B.; Johnson, T.; Jousilahti, P.; Jovanovic, Z.; Khaw, K. T.; Kraft, P.; Kuokkanen, M.; Kuusisto, J.; Laitinen, J.; Lakatta, E. G.; Luan, J.; Luben, R. N.; Mangino, M.; McArdle, W. L.; Meitinger, T.; Mulas, A.; Munroe, P. B.; Narisu, N.; Ness, A. R.; Northstone, K.; O'Rahilly, S.; Purmann, C.; Rees, M. G.; Ridderstrale, M.; Ring, S. M.; Rivadeneira, F.; Ruokonen, A.; Sandhu, M. S.; Saramies, J.; Scott, L. J.; Scuteri, A.; Silander, K.; Sims, M. A.; Song, K.; Stephens, J.; Stevens, S.; Stringham, H. M.; Tung, Y. C.; Valle, T. T.; Van Duijn, C. M.; Vimalaswaran, K. S.; Vollenweider, P.; Waeber, G.; Wallace, C.; Watanabe, R. M.; Waterworth, D. M.; Watkins, N.; Witteman, J. C.; Zeggini, E.; Zhai, G.; Zillikens, M. C.; Altshuler, D.; Caulfield, M.

- J.; Chanock, S. J.; Farooqi, I. S.; Ferrucci, L.; Guralnik, J. M.; Hattersley, A. T.; Hu, F. B.; Jarvelin, M. R.; Laakso, M.; Mooser, V.; Ong, K. K.; Ouwehand, W. H.; Salomaa, V.; Samani, N. J.; Spector, T. D.; Tuomi, T.; Tuomilehto, J.; Uda, M.; Uitterlinden, A. G.; Wareham, N. J.; Deloukas, P.; Frayling, T. M.; Groop, L. C.; Hayes, R. B.; Hunter, D. J.; Mohlke, K. L.; Peltonen, L.; Schlessinger, D.; Strachan, D. P.; Wichmann, H. E.; McCarthy, M. I.; Boehnke, M.; Barroso, I.; Abecasis, G. R.; Hirschhorn, J. N. Six new loci associated with body mass index highlight a neuronal influence on body weight regulation. *Nat Genet* **2009**, *41*, 25-34.
12. Feng, N.; Young, S. F.; Aguilera, G.; Puricelli, E.; Adler-Wailes, D. C.; Sebring, N. G.; Yanovski, J. A. Co-occurrence of Two Partially Inactivating Polymorphisms of MC3R Is Associated With Pediatric-Onset Obesity. *Diabetes* **2005**, *54*, 2663-2667.
13. Yang, Z.; Tao, Y. X. Mutations in Melanocortin-3 Receptor Gene and Human Obesity. *Prog Mol Biol Transl Sci* **2016**, *140*, 97-129.
14. Chen, W.; Kelly, M. A.; Opitz-Araya, X.; Thomas, R. E.; Low, M. J.; Cone, R. D. Exocrine Gland Dysfunction in MC5-R-Deficient Mice: Evidence for Coordinated Regulation of Exocrine Gland Function by Melanocortin Peptides. *Cell* **1997**, *91*, 789-798.
15. Nakanishi, S.; Inoue, A.; Kita, T.; Nakamura, M.; Chang, A. C.; Cohen, S. N.; Numa, S. Nucleotide sequence of cloned cDNA for bovine corticotropin-beta-lipotropin precursor. *Nature* **1979**, *278*, 423-7.
16. Castrucci, A. M. L.; Hadley, M. E.; Sawyer, T. K.; Wilkes, B. C.; Al-Obeidi, F.; Staples, D. J.; de Vaux, A. E.; Dym, O.; Hintz, M. F.; Riehm, J. P.; Rao, K. R.; Hruby, V. J.  $\alpha$ -melanotropin: The minimal active sequence in the lizard skin bioassay. *General and Comparative Endocrinology* **1989**, *73*, 157-163.
17. Haskell-Luevano, C.; Sawyer, T. K.; Hendrata, S.; North, C.; Panahinia, L.; Stum, M.; Staples, D. J.; De Lauro Castrucci, A. M.; Hadley, M. E.; Hruby, V. J. Truncation studies of  $\alpha$ -melanotropin peptides identify tripeptide analogues exhibiting prolonged agonist bioactivity. *Peptides* **1996**, *17*, 995-1002.
18. Haskell-Luevano, C.; Holder, J. R.; Monck, E. K.; Bauzo, R. M. Characterization of Melanocortin NDP-MSH Agonist Peptide Fragments at the Mouse Central and Peripheral Melanocortin Receptors. *Journal of Medicinal Chemistry* **2001**, *44*, 2247-2252.
19. Ollmann, M. M.; Wilson, B. D.; Yang, Y.-K.; Kerns, J. A.; Chen, Y.; Gantz, I.; Barsh, G. S. Antagonism of Central Melanocortin Receptors in Vitro and in Vivo by Agouti-Related Protein. *Science* **1997**, *278*, 135-138.
20. Nijenhuis, W. A. J.; Oosterom, J.; Adan, R. A. H. AgRP(83–132) Acts as an Inverse Agonist on the Human-Melanocortin-4 Receptor. *Molecular Endocrinology* **2001**, *15*, 164-171.
21. Wilczynski, A.; Wang, X. S.; Joseph, C. G.; Xiang, Z.; Bauzo, R. M.; Scott, J. W.; Sorensen, N. B.; Shaw, A. M.; Millard, W. J.; Richards, N. G.; Haskell-Luevano, C. Identification of Putative Agouti-Related Protein(87–132)-Melanocortin-4 Receptor Interactions by Homology Molecular Modeling and Validation Using Chimeric Peptide Ligands. *Journal of Medicinal Chemistry* **2004**, *47*, 2194-2207.
22. Joseph, C. G.; Wang, X. S.; Scott, J. W.; Bauzo, R. M.; Xiang, Z.; Richards, N. G.; Haskell-Luevano, C. Stereochemical Studies of the Monocyclic Agouti-Related Protein (103–122) Arg-Phe-Phe Residues: Conversion of a Melanocortin-4 Receptor Antagonist into an Agonist and Results in the Discovery of a Potent and Selective Melanocortin-1 Agonist. *Journal of Medicinal Chemistry* **2004**, *47*, 6702-6710.
23. Irani, B. G.; Xiang, Z.; Yarandi, H. N.; Holder, J. R.; Moore, M. C.; Bauzo, R. M.; Proneth, B.; Shaw, A. M.; Millard, W. J.; Chambers, J. B.; Benoit, S. C.; Clegg, D. J.; Haskell-Luevano, C. Implication of the melanocortin-3 receptor in the regulation of food intake. *European journal of pharmacology* **2011**, *660*, 80-87.

24. Hagan, M. M.; Rushing, P. A.; Pritchard, L. M.; Schwartz, M. W.; Strack, A. M.; Van der Ploeg, L. H. T.; Woods, S. C.; Seeley, R. J. Long-term orexigenic effects of AgRP-(83–132) involve mechanisms other than melanocortin receptor blockade. *American Journal of Physiology - Regulatory, Integrative and Comparative Physiology* **2000**, *279*, R47-R52.
25. Atalayer, D.; Robertson, K. L.; Haskell-Luevano, C.; Andreasen, A.; Rowland, N. E. Food demand and meal size in mice with single or combined disruption of melanocortin type 3 and 4 receptors. *American Journal of Physiology - Regulatory, Integrative and Comparative Physiology* **2010**, *298*, R1667-R1674.
26. Van der Ploeg, L. H. T.; Martin, W. J.; Howard, A. D.; Nargund, R. P.; Austin, C. P.; Guan, X.; Drisko, J.; Cashen, D.; Sebat, I.; Patchett, A. A.; Figueroa, D. J.; DiLella, A. G.; Connolly, B. M.; Weinberg, D. H.; Tan, C. P.; Palyha, O. C.; Pong, S.-S.; MacNeil, T.; Rosenblum, C.; Vongs, A.; Tang, R.; Yu, H.; Sailer, A. W.; Fong, T. M.; Huang, C.; Tota, M. R.; Chang, R. S.; Stearns, R.; Tamvakopoulos, C.; Christ, G.; Drazen, D. L.; Spar, B. D.; Nelson, R. J.; MacIntyre, D. E. A role for the melanocortin 4 receptor in sexual function. *Proceedings of the National Academy of Sciences of the United States of America* **2002**, *99*, 11381-11386.
27. Ni, X. P.; Butler, A. A.; Cone, R. D.; Humphreys, M. H. Central receptors mediating the cardiovascular actions of melanocyte stimulating hormones. *J Hypertens* **2006**, *24*, 2239-46.
28. Versteeg, D. H. G.; Van Bergen, P.; Adan, R. A. H.; De Wildt, D. J. Melanocortins and cardiovascular regulation. *European Journal of Pharmacology* **1998**, *360*, 1-14.
29. Hill, C.; Dunbar, J. C. The effects of acute and chronic alpha melanocyte stimulating hormone ( $\alpha$ MSH) on cardiovascular dynamics in conscious rats. *Peptides* **2002**, *23*, 1625-1630.
30. Greenfield, J. R.; Miller, J. W.; Keogh, J. M.; Henning, E.; Satterwhite, J. H.; Cameron, G. S.; Astruc, B.; Mayer, J. P.; Brage, S.; See, T. C.; Lomas, D. J.; O'Rahilly, S.; Farooqi, I. S. Modulation of Blood Pressure by Central Melanocortinergic Pathways. *New England Journal of Medicine* **2009**, *360*, 44-52.
31. Joseph, C. G.; Yao, H.; Scott, J. W.; Sorensen, N. B.; Marnane, R. N.; Mountjoy, K. G.; Haskell-Luevano, C.  $\gamma$ 2-Melanocyte stimulation hormone ( $\gamma$ 2-MSH) truncation studies results in the cautionary note that  $\gamma$ 2-MSH is not selective for the mouse MC3R over the mouse MC5R. *Peptides* **2010**, *31*, 2304-2313.
32. Collet, T.-H.; Dubern, B.; Mokrosinski, J.; Connors, H.; Keogh, J. M.; Mendes de Oliveira, E.; Henning, E.; Poitou-Bernert, C.; Oppert, J.-M.; Tounian, P.; Marchelli, F.; Alili, R.; Le Beyec, J.; Pépin, D.; Lacorte, J.-M.; Gottesdiener, A.; Bounds, R.; Sharma, S.; Folster, C.; Henderson, B.; O'Rahilly, S.; Stoner, E.; Gottesdiener, K.; Panaro, B. L.; Cone, R. D.; Clément, K.; Farooqi, I. S.; Van der Ploeg, L. H. T. Evaluation of a melanocortin-4 receptor (MC4R) agonist (Setmelanotide) in MC4R deficiency. *Molecular Metabolism* **2017**, *6*, 1321-1329.
33. Grieco, P.; Lavecchia, A.; Cai, M.; Trivedi, D.; Weinberg, D.; MacNeil, T.; Van der Ploeg, L. H. T.; Hruby, V. J. Structure–Activity Studies of the Melanocortin Peptides: Discovery of Potent and Selective Affinity Antagonists for the hMC3 and hMC4 Receptors. *Journal of Medicinal Chemistry* **2002**, *45*, 5287-5294.
34. Mayorov, A. V.; Cai, M.; Palmer, E. S.; Dedek, M. M.; Cain, J. P.; Van Scoy, A. R.; Tan, B.; Vagner, J.; Trivedi, D.; Hruby, V. J. Structure–Activity Relationships of Cyclic Lactam Analogues of  $\alpha$ -Melanocyte-Stimulating Hormone ( $\alpha$ -MSH) Targeting the Human Melanocortin-3 Receptor. *Journal of medicinal chemistry* **2008**, *51*, 187-195.
35. Carotenuto, A.; Merlino, F.; Cai, M.; Brancaccio, D.; Yousif, A. M.; Novellino, E.; Hruby, V. J.; Grieco, P. Discovery of Novel Potent and Selective Agonists at the Melanocortin-3 Receptor. *Journal of Medicinal Chemistry* **2015**, *58*, 9773-9778.

36. Grieco, P.; Balse, P. M.; Weinberg, D.; MacNeil, T.; Hruby, V. J. D-Amino acid scan of gamma-melanocyte-stimulating hormone: importance of Trp(8) on human MC3 receptor selectivity. *J Med Chem* **2000**, *43*, 4998-5002.
37. Doering, S. R.; Freeman, K. T.; Schnell, S. M.; Haslach, E. M.; Dirain, M.; Debevec, G.; Geer, P.; Santos, R. G.; Giulianotti, M. A.; Pinilla, C.; Appel, J. R.; Speth, R. C.; Houghten, R. A.; Haskell-Luevano, C. Discovery of Mixed Pharmacology Melanocortin-3 Agonists and Melanocortin-4 Receptor Tetrapeptide Antagonist Compounds (TACOs) Based on the Sequence Ac-Xaa1-Arg-(p)DPhe-Xaa4-NH<sub>2</sub>. *Journal of Medicinal Chemistry* **2017**, *60*, 4342-4357.
38. Doering, S. R.; Todorovic, A.; Haskell-Luevano, C. Melanocortin Antagonist Tetrapeptides with Minimal Agonist Activity at the Mouse Melanocortin-3 Receptor. *ACS Medicinal Chemistry Letters* **2015**, *6*, 123-127.
39. Houghten, R. A.; Pinilla, C.; Appel, J. R.; Blondelle, S. E.; Dooley, C. T.; Eichler, J.; Nefzi, A.; Ostresh, J. M. Mixture-Based Synthetic Combinatorial Libraries. *Journal of Medicinal Chemistry* **1999**, *42*, 3743-3778.
40. Houghten, R. A.; Pinilla, C.; Giulianotti, M. A.; Appel, J. R.; Dooley, C. T.; Nefzi, A.; Ostresh, J. M.; Yu, Y.; Maggiora, G. M.; Medina-Franco, J. L.; Brunner, D.; Schneider, J. Strategies for the Use of Mixture-Based Synthetic Combinatorial Libraries: Scaffold Ranking, Direct Testing In Vivo, and Enhanced Deconvolution by Computational Methods. *Journal of Combinatorial Chemistry* **2008**, *10*, 3-19.
41. Haslach, E. M.; Huang, H.; Dirain, M.; Debevec, G.; Geer, P.; Santos, R. G.; Giulianotti, M. A.; Pinilla, C.; Appel, J. R.; Doering, S. R.; Walters, M. A.; Houghten, R. A.; Haskell-Luevano, C. Identification of tetrapeptides from a mixture based positional scanning library that can restore nM full agonist function of the L106P, I69T, I102S, A219V, C271Y, and C271R human melanocortin-4 polymorphic receptors (hMC4Rs). *J Med Chem* **2014**, *57*, 4615-28.
42. Holder, J. R.; Bauzo, R. M.; Xiang, Z.; Haskell-Luevano, C. Structure-activity relationships of the melanocortin tetrapeptide Ac-His-DPhe-Arg-Trp-NH<sub>2</sub> at the mouse melanocortin receptors: part 2 modifications at the Phe position. *J Med Chem* **2002**, *45*, 3073-81.
43. Carpino, L. A.; Han, G. Y. 9-Fluorenylmethoxycarbonyl amino-protecting group. *The Journal of Organic Chemistry* **1972**, *37*, 3404-3409.
44. Merrifield, R. B. Solid Phase Peptide Synthesis. I. The Synthesis of a Tetrapeptide. *Journal of the American Chemical Society* **1963**, *85*, 2149-2154.
45. Kaiser, E.; Colescott, R. L.; Bossinger, C. D.; Cook, P. I. Color test for detection of free terminal amino groups in the solid-phase synthesis of peptides. *Anal Biochem* **1970**, *34*, 595-8.
46. Vojkovsky, T. Detection of secondary amines on solid phase. *Pept Res* **1995**, *8*, 236-7.
47. Hoehn, R. D.; Nichols, D. E.; McCorvy, J. D.; Neven, H.; Kais, S. Experimental evaluation of the generalized vibrational theory of G protein-coupled receptor activation. *Proc Natl Acad Sci U S A* **2017**, *114*, 5595-5600.
48. Chen, C. A.; Okayama, H. Calcium phosphate-mediated gene transfer: a highly efficient transfection system for stably transforming cells with plasmid DNA. *Biotechniques* **1988**, *6*, 632-8.
49. Kaminski, G. A.; Friesner, R. A.; Tirado-Rives, J.; Jorgensen, W. L. Evaluation and Reparametrization of the OPLS-AA Force Field for Proteins via Comparison with Accurate Quantum Chemical Calculations on Peptides. *The Journal of Physical Chemistry B* **2001**, *105*, 6474-6487.
50. Chen, W.; Shields, T. S.; Stork, P. J.; Cone, R. D. A colorimetric assay for measuring activation of Gs- and Gq-coupled signaling pathways. *Anal Biochem* **1995**, *226*, 349-54.
51. Proneth, B.; Pogozeva, I. D.; Portillo, F. P.; Mosberg, H. I.; Haskell-Luevano, C. Melanocortin Tetrapeptide Ac-His-DPhe-Arg-Trp-NH<sub>2</sub> Modified at the Para Position of the

Benzyl Side Chain (DPhe): Importance for Mouse Melanocortin-3 Receptor Agonist versus Antagonist Activity. *Journal of Medicinal Chemistry* **2008**, 51, 5585-5593.

52. Wilczynski, A.; Wang, X. S.; Joseph, C. G.; Xiang, Z.; Bauzo, R. M.; Scott, J. W.; Sorensen, N. B.; Shaw, A. M.; Millard, W. J.; Richards, N. G.; Haskell-Luevano, C. Identification of putative agouti-related protein(87-132)-melanocortin-4 receptor interactions by homology molecular modeling and validation using chimeric peptide ligands. *J Med Chem* **2004**, 47, 2194-207.

53. Fleck, B. A.; Chen, C.; Yang, W.; Huntley, R.; Markison, S.; Nickolls, S. A.; Foster, A. C.; Hoare, S. R. Molecular interactions of nonpeptide agonists and antagonists with the melanocortin-4 receptor. *Biochemistry* **2005**, 44, 14494-508.

54. Nickolls, S. A.; Cismowski, M. I.; Wang, X.; Wolff, M.; Conlon, P. J.; Maki, R. A. Molecular Determinants of Melanocortin 4 Receptor Ligand Binding and MC4/MC3 Receptor Selectivity. *Journal of Pharmacology and Experimental Therapeutics* **2003**, 304, 1217-1227.

55. Schild, H. O. pA, a new scale for the measurement of drug antagonism. *British journal of pharmacology and chemotherapy* **1947**, 2, 189-206.